Rainfall over the Maritime Continent: key processes, scale interactions and model representation

Ashar A. Aslam
School of Earth and Environment, University of Leeds, UK

Introduction

The Maritime Continent (MC) refers to thousands of islands and many shallow seas in southeast Asia (Figure 1a). The MC experiences heavy rainfall and deep convection all year round (Figures 1b–e): a product of the high sea surface temperatures (SSTs) and variable topography characterising the region. Regional rainfall is observed to be twice that of the global mean (Yamanaka *et al*., 2018). Through the latent heat release associated with intense rainfall and convection, the MC forms a key component of the global weather and climate system. Atmospheric circulation and climate are influenced through the generation of Rossby waves and the subsequent propagation of these waves towards the extratropics (Jin and Hoskins, 1995).

On seasonal-to-annual timescales, rainfall patterns are modulated by the monsoon circulation, driven by shifts in the Intertropical Convergence Zone (ITCZ, Figures 1b–e). Across the MC, there tends to be more rainfall in the boreal winter (December–February, or DJF) and lower amounts in the boreal summer (June–August, or JJA; e.g. As-syakur *et al*., 2013). However, many additional processes influence the environmental state within the MC, modulating regional patterns in convection (Yamanaka, 2016). These processes operate over a wide range of scales, from larger-scale modes of variability to more local and transient variability regulated by finer-scale processes. In addition, there are scale interactions, as well as geographical variability in responses to forcings, which complicate our understanding of the MC environment further. The intensity of rainfall experienced causes many detrimental impacts, such as flooding and landslides, which can lead to significant health crises and losses (Torti, 2012; Wijayanti *et al*., 2017).

With a population of over 500 million people residing across the MC, better understanding the processes which govern the regional rainfall patterns is crucial. However, weather stations, providing key ground-based observations, are scarce and unevenly distributed across the MC (Koh and Teo, 2009). Therefore, we rely on broader-scale observations such as from satellites, as well as regional-to-local-scale climate models to improve our understanding. Conducting more extensive research into the meteorology of the region will help to improve flood forecasting systems and other solutions for minimising regional vulnerability to disaster and emergency.

In this review, I provide a concise overview of the key features related to the severe weather observed across the MC, and highlight both the growth in knowledge and remaining gaps. I first outline processes well-understood to impact MC rainfall in the 'Key processes' section, with an exploration of the various scale interactions that exist between some of these processes in the 'Scale interactions' section. In the 'Model representation' section, I address the ability of current state-of-the-art weather and climate models in representing these processes, and any deficiencies that have persisted, including where improvements are needed, in addition to future climate projections of MC rainfall.

Key processes

The MC experiences rainfall all year round and several processes regulate regional precipitation patterns. The background environmental state of the MC is modulated by large-scale modes of variability, with local and more transient variability regulated by finer-scale processes. These processes are described in schematic form in Figure 2.

Interannual variability: El Niño Southern Oscillation and Indian Ocean Dipole

The El Niño Southern Oscillation (ENSO) is one of the two modes of variability influencing the MC on interannual timescales (e.g. McPhaden *et al*., 2006). ENSO consists of two phases – El Niño and La Niña – which each have different broad impacts on rainfall in the MC (e.g. Haylock and McBride, 2001; Rauniyar and Walsh, 2013). The large-scale circulation associated with ENSO consists of a strengthened Walker circulation over the MC during La Niña. This circulation is weakened during El Niño. Changes to circulations are modulated by SSTs in the central-eastern tropical Pacific, with warmer SSTs linked to El Niño and colder SSTs linked to La Niña. Equatorial easterlies weaken during El Niño, shifting the preferential location of convection further east, which results in reduced large-scale rainfall (negative anomalies of up to around 3mm day^{-1} relative to climatology) over the MC (Figure 3a). La Niña results in strengthening equatorial easterlies and large-scale ascent over the MC, enhancing large-scale rainfall (positive anomalies of up to around 3mm day^{-1} relative to climatology), shown in Figures 2(a) and 3(b). These relationships are more distinct in the dry season (Hendon, 2003), however Jia *et al*. (2016) highlight that for strong El Niño and La Niña events in the wintertime, rainfall is reduced and enhanced, respectively, in the northern and eastern MC by up to 5mm day^{-1}.

The Indian Ocean Dipole (IOD) is another mode of variability important on interannual timescales (e.g. Saji *et al*., 1999; Saji and Yamagata, 2003), and has similar phases to ENSO. During the positive IOD, high and low SSTs are observed in the western and eastern Indian Ocean, respectively. The converse applies to the negative IOD. These SSTs produce a Walker-like circulation with enhanced easterlies across the Indian Ocean during the positive IOD, leading to enhanced descent over the MC and uplift over eastern Africa. Suppression of rainfall is primarily observed over the western portion of the MC during this phase (Figure 3c). The negative IOD has a circulation opposite to that of the positive IOD. Therefore, the negative IOD favours an increase in rainfall over the MC, as displayed in Figure 2(a) alongside the La Niña signal originating from the Pacific, though rainfall enhancement is primarily observed from the southwestern MC to mainland southeast Asia (Figure 3d).

Weather – 9999, Vol. 99, No. 9

RMetS Royal Meteorological Society

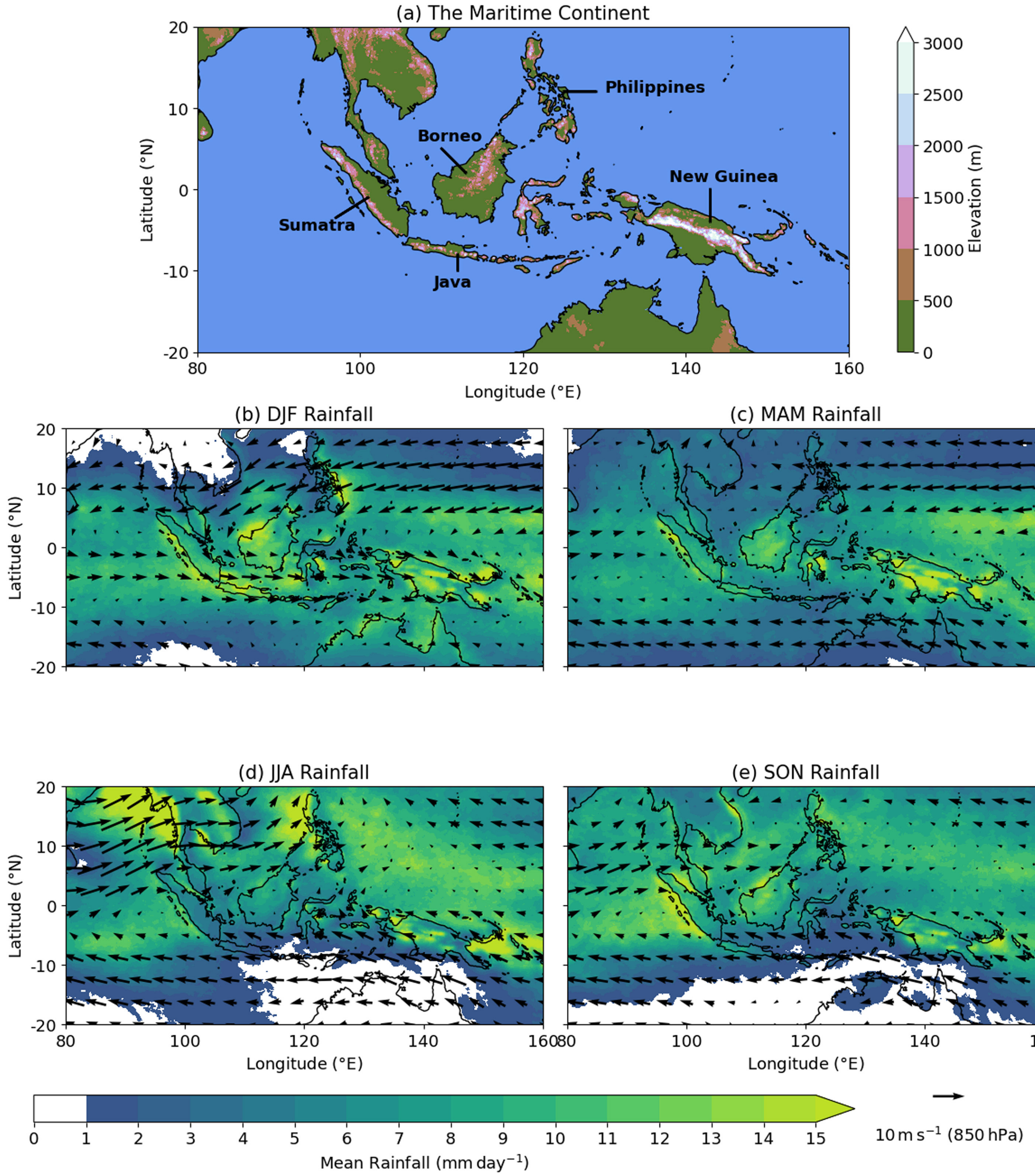

Figure 1. (a) Map showing the topography of the Maritime Continent, with some of the constituent islands labelled. Panels (b), (c), (d) and (e) show the climatological means of IMERG GPM (Huffman et al.*, 2020) precipitation rates for December–February (DJF), March–May (MAM), June–August (JJA), and September–November (SON) respectively, from 20 years of data from December 2000 to November 2020. Black arrows represent mean ERA5 (Hersbach* et al.*, 2020) 850hPa wind for the equivalent time period.*

Intraseasonal variability: Madden–Julian Oscillation

The Madden–Julian Oscillation (MJO, Figure 2b) is the main source of intraseasonal variability in the Tropics, with a long-period oscillation of roughly 30–90 days (e.g. Madden and Julian, 1994). Wheeler and Hendon (2004) derived eight MJO phases through empirical orthogonal function analysis of top-of-atmosphere outgoing longwave radiation and zonal wind at 850 and 200hPa. These phases describe the eastward propagation of the active, or convective, phase of the MJO through the tropical warm pool from the Indian Ocean to the West Pacific. The active (suppressed) envelope can be characterised by rainfall anomalies exceeding ±5mm day^{-1} in regions, relative to climatology (Figures 3e–l). Applying the convention of Wheeler and Hendon, the active phase of the MJO is observed over the MC during Phases 4–5. Over the MC, Liang *et al.* (2022) showed that the MJO can be attributed to around 60% of total rainfall, and 50% of total extreme rainfall.

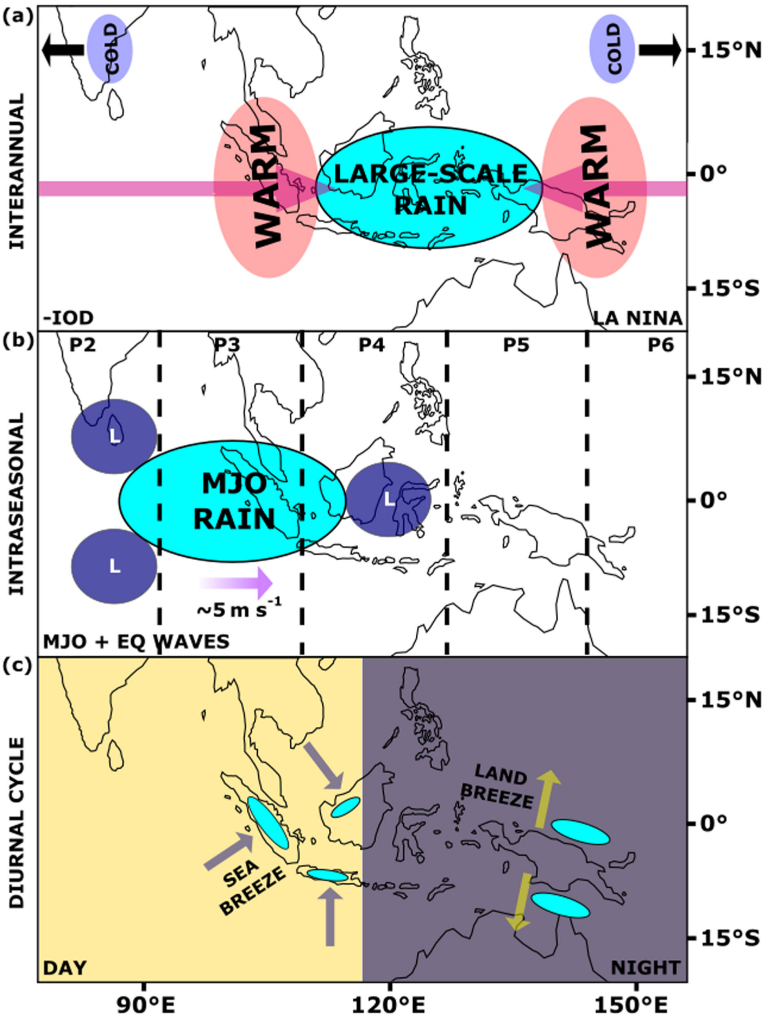

Figure 2. A set of schematics briefly summarising various processes which influence rainfall patterns over the Maritime Continent. These are at (a) interannual timescales, associated with the Indian Ocean Dipole (IOD) and El Niño Southern Oscillation (ENSO, shown for their respective negative phases), (b) intraseasonal timescales, associated with the Madden–Julian Oscillation (MJO) and equatorial waves and (c) diurnal timescales, associated with land-sea breeze dynamics. In (b), labels at the top of the panel highlight approximate geographical locations in which the MJO is active at each phase. In (c), cyan ovals are as in (a) and (b) but for rainfall associated with diurnal convective propagation.

The MJO propagates at a speed of around 5ms^{-1} as SSTs and induced surface heat fluxes help to prime the atmosphere to the east for further convection, at a feedback timescale of around 7 days, suppressing convection to the west (Hendon and Glick, 1997; Woolnough *et al*., 2000, 2001; Zhang, 2005). Several theories attempt to explain MJO propagation, as outlined in a thorough review by Zhang *et al*. (2020).

One key theory involves moisture modes, where MJO propagation is dictated by tropical moisture anomalies (e.g. Adames and Maloney, 2021). Instability to this mode occurs when precipitation is a strongly increasing function of saturation in the tropical atmosphere (Raymond and Fuchs, 2009). This instability is non-linear, enhanced by surface flux and cloud-radiative feedbacks, moist advection and convergence, and shifts in the phasing of wind and precipitation, which can affect both MJO propagation, the structure of the associated moisture field, and the role of equatorial waves (e.g. Sobel and Maloney, 2013; Adames and Wallace, 2015; Chen and Wang, 2019; Wang and Li, 2020).

Synoptic-scale inertial gravity waves embedded within the MJO are also thought to enable eastward propagation (e.g. Yang and Ingersoll, 2013). The theory does not explicitly incorporate moisture, other than in enabling precipitation to occur once convective instability has developed. Convection can help to excite gravity waves to transport mass away from convection, producing a cycle of convective excitation. Other studies also suggest the active envelope consists of both mesoscale and synoptic-scale components (Majda and Stechmann, 2009), thereby challenging the canonical view of the MJO being a purely large-scale mode.

MJO characteristics have also been related to equatorial wave dynamics (e.g. Hendon and Salby, 1994; Maloney and Hartmann, 1998; Matthews, 2000). During the active phase of the MJO, a tongue of low pressure strengthens to the east, associated with a Kelvin wave, with pressure troughs to the northwest and southwest, associated with Rossby waves (Matsuno, 1966; Gill, 1980) The opposite is observed for the suppressed phase of the MJO. Through this hypothesis, MJO physics can be related to the feedbacks between these dynamics and the moist properties of the large-scale convective field (Wang *et al*., 2016).

Equatorial waves

Equatorial waves, previously described in relationship to MJO properties, have theoretical structures described by solutions to the shallow water equations (e.g. Matsuno, 1966; Gill, 1980). Examples of equatorial waves include Kelvin (eastward-moving with no meridional velocity component), mixed Rossby-gravity (non-zero meridional velocity, with eastward- and westward-moving solutions) and equatorial Rossby waves (westward-moving). These waves are trapped near the Equator due to poleward reductions in the magnitude of the Coriolis force and can be excited by processes such as diabatic heating of the tropical atmosphere.

As shown by filtered satellite observations of outgoing longwave radiation (Wheeler and Kiladis, 1999), equatorial waves help to organise and can couple with tropical convection on synoptic to sub-seasonal timescales, thereby affecting the probability of rainfall. Ridout and Flatau (2011), for example, show that these waves are key in shifting regions of low-level moisture convergence. Significant increases in extreme precipitation can be observed when high amplitude waves are present over the MC. Senior *et al*. (2023) found extreme precipitation may be around 60% more likely when convectively coupled Kelvin waves are observed over western Sumatra. Latos *et al*. (2021) found extreme rainfall to be twice as likely over Sulawesi when these waves are present, and up to eight times as likely if there is additional activity from other equatorial waves. Ferrett *et al*. (2020) found extreme precipitation over the broader MC can be up to four times more likely in the presence of high amplitude waves. However, each wave has a spatially variable degree of influence on rainfall patterns across the MC (Yang *et al*., 2003; Ferrett *et al*., 2020; Peatman *et al*., 2021).

Diurnal cycle

The diurnal cycle is the most fundamental process controlling variability in convec-

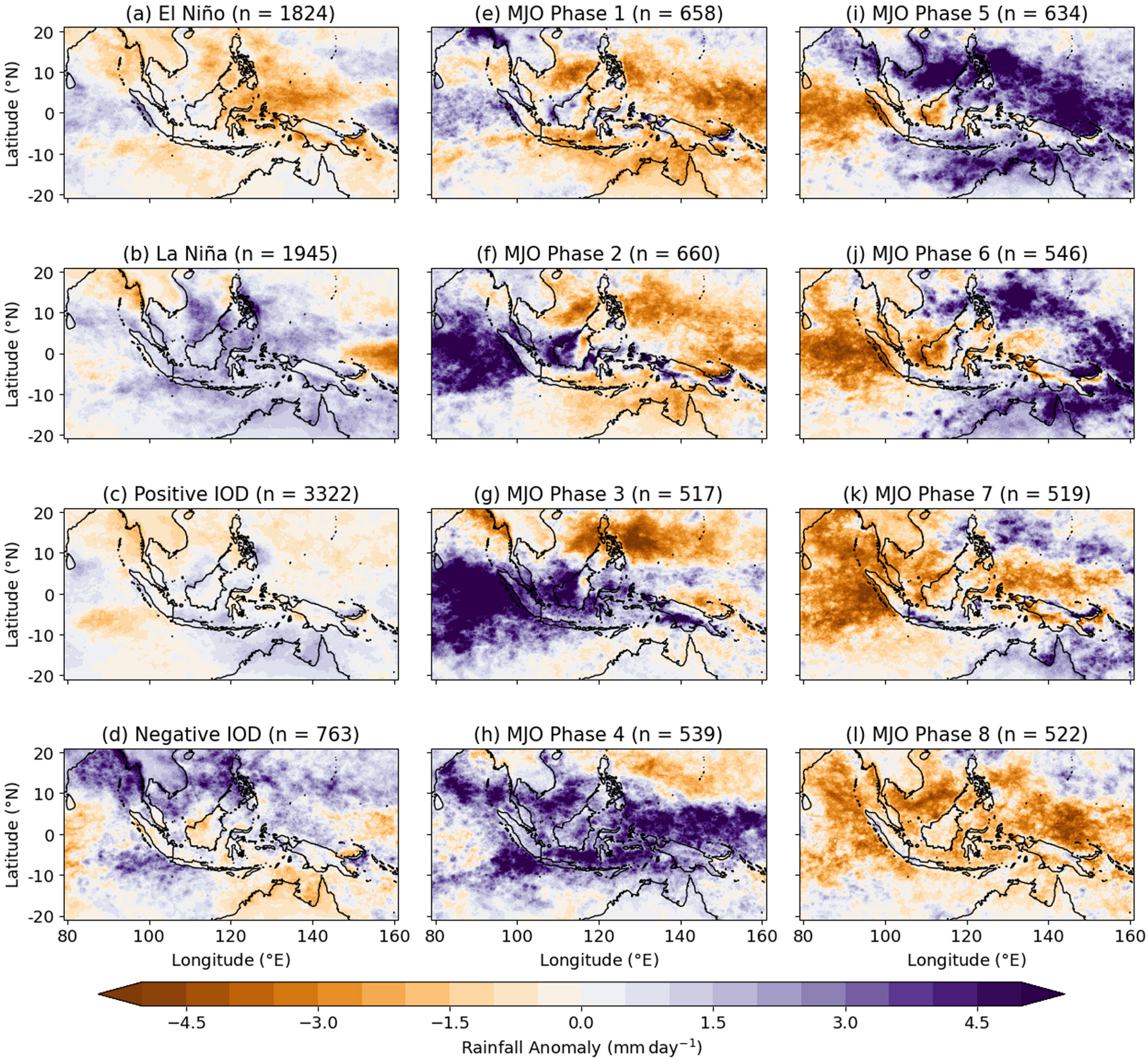

Figure 3. Rainfall anomalies over the Maritime Continent for (a, b) the El Niño and La Niña phases of ENSO, (c, d) the positive and negative phases of the IOD and (e–l) the eight phases of the MJO, as described by Wheeler and Hendon (2004). These anomalies are relative to the mean across 20 years of GPM rainfall from December 2000 to November 2020. Values of n *represent the number of days within each of the phases, over which composites are constructed. See the 'Data Availability Statement' for phase definitions.*

tion over the MC on local scales, modulated by complex land-sea interactions (e.g. Yang and Slingo, 2001). These interactions develop initially through daytime insolation, where increased warming of the land relative to the ocean, due to differences in heat capacity, sets up a land-sea temperature contrast. This contrast forces sea breeze convergence onto land, through the induced pressure gradient, and upslope mountain winds, forming deep convection and precipitation into the afternoon and evening inland/on mountain flanks (Qian, 2008). Overnight, the land cools more rapidly than the ocean, reversing the pressure gradient, forming land breezes and downslope mountain winds, and in some cases, resulting in offshore propagation of the convection that formed overland. These processes are depicted in Figure 2(c).

However, mechanisms associated with the propagation of convection offshore overnight remain an active area of research. Authors such as Mori *et al*. (2004) and Yokoi *et al*. (2017) provide thorough overviews of existing hypotheses. These include various interactions between the ambient wind, gravity waves, cloud structure, and thermal instability produced by diabatic processes over land (e.g. Satomura, 2000; Nesbitt and Zipser, 2003; Warner *et al*., 2003; Hassim *et al*., 2016; Peatman *et al*., 2023). Mori *et al*. (2004) and Yokoi *et al*. (2017) both state that offshore propagation and subsequent decay of convection over land is likely driven by a combination of these theories.

The diurnal cycle in rainfall is common to most islands in the MC, with a distinct diurnal peak in the maximum rainfall from the afternoon to the late evening over land, compared to the morning over the ocean (Figure 4). However, the impact of the diurnal cycle is variable across the region. For example, changes in wind regimes and circulations both day-on-day and over the MC can modulate the strength of the diurnal cycle over land, with additional higher-order components of variability influencing diurnal characteristics further (e.g. Peatman *et al*., 2021; Mustafa *et al*., 2024). Therefore, the role of the diurnal cycle cannot be generalised for the entire region.

Synoptic circulations

There are other well-documented processes which influence rainfall patterns in the MC; however, they operate on more variable and synoptic spatial and temporal scales. For example, cold surges are phenomena which form due to strengthened prevailing low-level northerly-to-northeasterly winds due to cold air outbreaks originating from the Siberian High (e.g. Koseki *et al*., 2013). Cold surges bring enhanced rainfall at their leading edges due to perturbing pre-existing monsoonal flow. Closely related to, and often induced by, cold surges are Borneo vortices (e.g. Hardy *et al*., 2023). These form in the later phases of the northeasterly monsoon over the South China Sea and are one of the main drivers of rainfall in regions such as Malaysia.

On top of these, tropical cyclones are also impactful in the MC. Tropical cyclones are well-known destructive weather systems with impacts felt worldwide – in the MC, compared to other processes, these systems tend to mostly detrimentally impact the northern MC, primarily in boreal summer, through induced precipitation and wind extremes (e.g. Takahashi, 2011; Li *et al*., 2022). Cyclones in this region have the potential to reduce larger-scale rainfall over the MC through changes to the wind field, leading to anomalous region-wide subsidence and moisture divergence (e.g. Scoccimarro *et al*., 2020; Li *et al*., 2024). Latos *et al*. (2023) identified that environmental spin-up driven by processes such as equatorial waves and the MJO can also cause unusual near-equatorial tropical cyclones to form.

Scale interactions

While various key processes have particular direct impacts on MC rainfall, additional interactions between them exist on a range of spatial and temporal scales. These interactions complicate our image of the meteorological patterns across the region.

MJO–diurnal cycle interactions

A well-known scale interaction exists between the MJO and the diurnal cycle. Generally, it is expected that the active (suppressed) envelopes of the MJO lead to increases (reductions) in large-scale rainfall over the MC. Oh *et al*. (2012) noted that the strong MJO winds and their interactions with monsoonal flow can however disrupt convergence, and therefore convective characteristics, over islands on diurnal timescales. Their study highlights a reduction in average land rainfall by around 0.5mmh^{-1} as the MJO active envelope passes over the MC from the Indian Ocean. Convergence may therefore be concentrated over the ocean, enhancing wind-induced surface heat exchange, though with a smaller increase in oceanic rainfall.

Additionally, Peatman *et al*. (2014) showed that a '*vanguard of precipitation*' jumps ahead of the active MJO envelope by one phase (around 6days) while the MJO is in its suppressed phase over the MC (depicted schematically in Figure 5). This phenomenon is influenced by the strong diurnal cycle over land, where changes in the amplitude of the diurnal cycle account for 80% of the changes in daily mean rainfall during an MJO cycle. Related to equatorial wave dynamics, frictional and topographic moisture convergence (driven by the eastward pressure gradient) and clear skies (destabilisation of the atmosphere through incoming insolation) ahead of the main convective envelope combine with the low thermal inertia of the land, allowing a rapid response to the diurnal cycle, moistening the environment to the east and enabling convection to develop. Thus, the islands act as a precipitation barrier to the smooth MJO propagation across the MC (e.g. Qian, 2008; Birch *et al*., 2016; Ajayamohan *et al*., 2021).

ENSO–diurnal cycle interaction

Similar to the MJO, ENSO interacts with the diurnal cycle. During El Niño, when there is suppressed convection over the MC, the diurnal cycle may be excited due to increased incoming solar radiation, giving precipitation anomalies of the opposite sign over the islands, relative to the ocean (Rauniyar and Walsh, 2013). Peatman *et al*. (2021) also deduced that, for Sumatra, on more local spatial scales, El Niño events exhibit a more offshore style of wind regime, leading to divergence in the MC lower-troposphere. The opposite is observed for La Niña, where heightened onshore flow can suppress the diurnal cycle by limiting seaward propagation of convection, reducing the contribution from diabatic effects over land.

Lu *et al*. (2023) observed opposite geographical relationships between modifications of the diurnal cycle amplitude between El Niño and La Niña. In their study, the amplitude is enhanced over the western MC and reduced over the east in El Niño, with the opposite findings for La Niña, attributed to shifts primarily in ENSO-regulated background moisture and convergence. However, diurnal winds were identified as being four times as important in modulating these interactions in the eastern MC, compared to the west. These findings emphasise the two-way interactions between the diurnal cycle and large-scale modes of variability.

Equatorial wave–diurnal cycle interactions

Equatorial waves also have the potential to interact with the diurnal cycle. Baranowski *et al*. (2016) showed that Kelvin waves can enhance island precipitation, as well as increase the probability of wave propagation across the MC, if they arrive in phase with the diurnal cycle. Sakaeda *et al*. (2020) found that Kelvin waves can also modulate the diurnal amplitude by modifying the lower-tropospheric wind field, thereby enhancing perturbations in moisture and

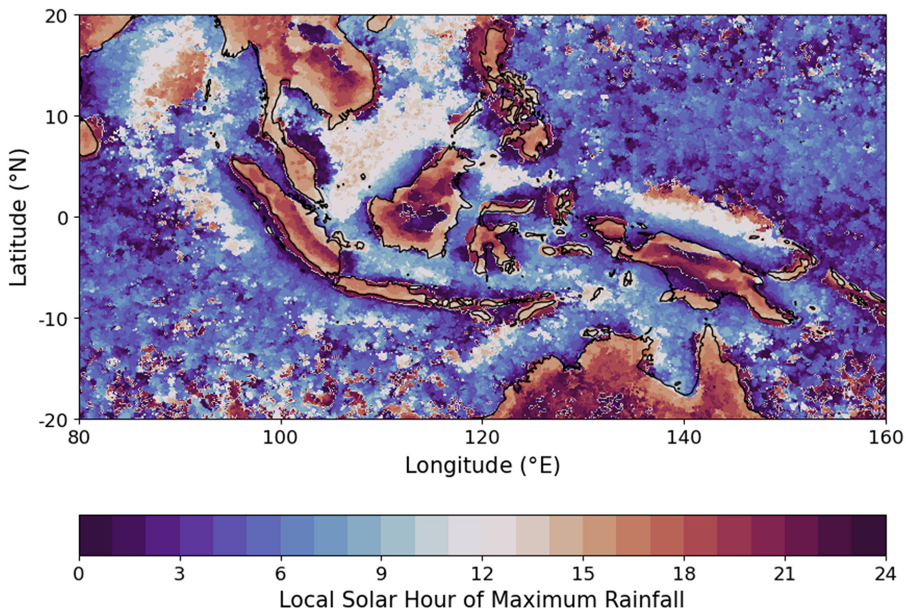

Figure 4. Local solar hour of maximum rainfall for each gridpoint across the entirety of the Maritime Continent, derived from the mean diurnal cycle of 20years of GPM rainfall from December 2000 to November 2020.

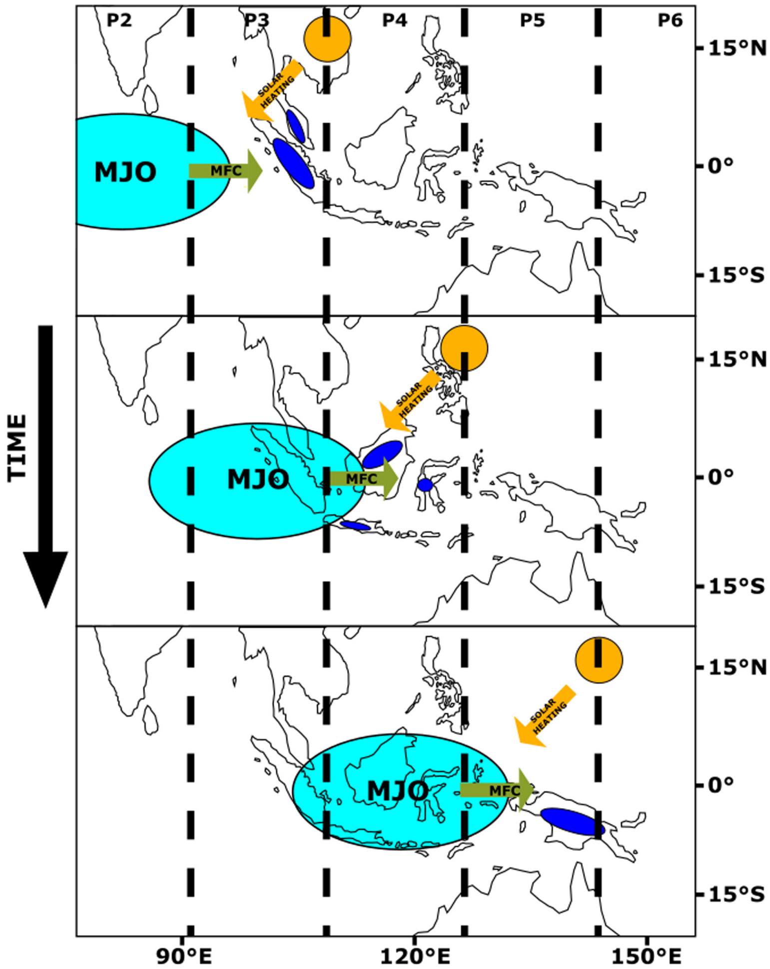

Figure 5. Schematic of a scale interaction between the MJO and the diurnal cycle. Convergence of moisture ahead of the active envelope combined with diurnal heating of the land leads to convection initiating around one phase ahead of the active envelope (dark blue ovals).

vertical motion over land. Geng *et al.* (2020) observed similar results for mixed Rossby-gravity waves.

Model representation

The observational network across the MC is constrained by both the number and distribution of meteorological stations (e.g. Koh and Teo, 2009), with the shallow bathymetry also limiting the potential for intensive ocean studies. These limitations feedback onto other datasets which depend on existing knowledge often obtained from observations. Weather and climate models, however, enable us to fine-tune parametrisation schemes and general model set-up to both capture processes better and to also test hypotheses in more idealised scenarios.

However, simulations of MC precipitation show many biases within models when compared to observations. The prediction of atmospheric and oceanic variables over the MC is challenging because of the complex regional geography and influences from remote forcings. Errors that persist within the MC have the potential to propagate globally through the induced Rossby waves originating from vertical heating over the region (Neale and Slingo, 2003; Qian, 2008; Love *et al.*, 2011). These features additionally feedback onto the way in which we accurately predict weather. Large-scale spatial variability in precipitation tends to have greater predictive skill than at more local scales (e.g. Ferrett *et al.*, 2021). Skill is inevitably dependent on the characterisation of key processes within models.

Resolution

Increasing horizontal model resolution has been shown to improve model performance through better representation of MC island geography and associated land–sea breeze circulations (e.g. Schiemann *et al.*, 2014; Rashid and Hirst, 2017). Neale and Slingo (2003) and Qian (2008) highlighted, through island-removal experiments, that under-representation of the complex geography of the MC and associated circulations/dynamics can alter simulated rainfall by around 15%. Tan *et al.* (2021) found that by varying which island was removed in sensitivity experiments can significantly impact the role of the lower-tropospheric zonal winds in modulating the magnitude and sign of moisture convergence and rainfall intensity over neighbouring islands.

Inclusion of the islands can help to improve interactions with larger-scale modes of variability (Holloway *et al.*, 2013), whilst making responses of convection to island-specific processes, such as gravity wave forcing, more realistic (Love *et al.*, 2011). Precipitation sensitivity to complex orography is reduced, thereby confining wet biases over smaller areas (Argüeso *et al.*, 2020).

However, studies have emphasised that changes in resolution are only effective at the coarsest scales, up to a 'threshold' (e.g. Pearson *et al.*, 2014). In global climate models, Neale and Slingo (2003) state a threefold increase in horizontal resolution is still insufficient to resolve diurnal processes. Rainfall can become too strong at higher resolution, with poor timings in the diurnal cycle over the islands (Li *et al.*, 2017). Therefore, some processes still remain unresolved even with fining of horizontal grid spacing.

Parametrisation

With increases in computing power, convection-permitting models (CPMs), where convection is represented explicitly, are shown to better resolve both rainfall and the land-sea breeze circulations (e.g. Birch *et al.*, 2016). These CPMs provide more realistic temperature and moisture tendencies compared to their parameterised counterparts (Holloway *et al.*, 2012).

However, while CPMs agree with existing hypotheses such as the impacts of the diurnal cycle on rainfall and improving characteristics of spatially heterogeneous features, biases persist. In particular, these issues are often linked to diurnal rainfall characteristics, with potential for overestimation of land-based precipitation and feedbacks onto large-scale modes of variability (e.g. Birch *et al.*, 2016; Hassim *et al.*, 2016; Vincent and Lane, 2016; Ajayamohan *et al.*, 2021).

These findings imply unresolved processes that require parametrisation remain. Further modification of parameterised processes can also help, such as through cloud property schemes and prescribed ocean conditions (e.g. Su *et al.*, 2022; Okugawa *et al.*, 2024). However, fundamental issues in employed model physical parametrisations, which represent sub-grid processes, are linked to limitations in current knowledge.

Coupling

Xue *et al.* (2020) produced a review on the role of coupling in modelling studies across the MC, highlighting that there are unresolved physical processes and inadequate representation of the ocean–atmosphere system, which can be alleviated by the introduction of coupling. Coupling is beneficial in managing atmospheric-ocean feedbacks, such as those related to SSTs, heat fluxes, wind and moisture, which can correct deficiencies in intraseasonal variability in precipitation (Pegion and Kirtman, 2008; Klingaman and Woolnough, 2014; DeMott *et al.*, 2019).

A more diurnal representation of SSTs when implementing coupling is increasingly preferable (e.g. Bernie *et al.*, 2007). Diurnal rectification and air-sea feedbacks induced by sub-daily coupling can result in more accurate diurnal evolutions of convection, while also improving mean state SST and precipitation distributions (Bernie *et al.*, 2008; Li *et al.*, 2020).

This imposed diurnal SST is, however, sensitive to vertical resolution. By mixing the upper ocean to various depths to simulate coarsened vertical resolution, Karlowska *et al.* (2024) noted weakened diurnal SST variability; thereby, in their study, weakening the feedback with the MJO and reducing regional rainfall. Similarly, Ma and Jiang (2021) found increased vertical resolution warmed the surface ocean, helping to enhance moisture gradients and convergence, convective instability and vertical circulations to the east of the active envelope, strengthening MJO propagation.

However, mean biases in the environmental state can affect the sensitivity to coupling (Klingaman and DeMott, 2020). Coupling may be insufficient to fully correct mean-state biases, which remain reliant on model configuration, including parametrisations and imposed sensitivities (Klingaman and Woolnough, 2014; DeMott *et al.*, 2019; Li *et al.*, 2020).

Future projections

Our modelling capabilities of the present climate inform our projections for the future. As the MC already experiences extreme rainfall regulated by processes operating over a wide range of spatial and temporal scales, it is important to assess how these patterns may change with global warming. Models can help extend inferences gained from observational analysis of rainfall trends over recent decades, both spatially and temporally, given these may tend to be very location-specific (e.g. Li *et al.*, 2018).

Various studies as part of CORDEX (Coordinated Regional Climate Downscaling Experiment) aimed to provide climate information at finer spatial resolutions, using dynamical downscaling to capture more regional and synoptic variability (e.g. Supari Tangang *et al.*, 2020; Tangang *et al.*, 2020; Ngai *et al.*, 2022). By analysing various indices reflective of both wet and dry extremes, these studies find reductions in mean future rainfall of up to 30% in boreal summer, primarily across Indonesia. In boreal winter, equivalent increases are observed over the northern MC and mainland Indochina. These results were noted to be due to changes to the monsoonal circulation and the associated moisture convergence in the future climate.

Kang *et al.* (2019), through application of CMIP5 scenarios to regional climate model projections, found a significant decrease in intermonsoon rainfall, linked to shifts in the regional meridional circulation. Hsu *et al.* (2025) observed an amplification of wet and dry extremes with global warming, driven by solely dynamic processes, and combined moist thermodynamic and dynamic processes, respectively.

Studies have also highlighted (extreme) rainfall may be modulated by shifts in larger-scale forcing (Liang *et al.*, 2022). Chen *et al.* (2023) found an eastward shift in the ENSO-related rainfall dipole across the MC in the dry season, with additional amplifications of the drying (wetting) commonly associated with El Niño (La Niña). Ghosh and Shepherd (2023) found, using CMIP6 scenarios, similarly strong changes in dry season rainfall driven by shifts in the forcings associated with both basin-wide warming and the equatorial SST gradient across the Pacific Ocean, tied to ENSO.

While Chen *et al.* (2023) reported that even historically biased models do not have significantly different future projections, uncertainty across ensemble members will persist. Each member, in isolation, will have varying ability to successfully capture key processes highlighted, or alluded to, in the 'Resolution', 'Parametrisation', and 'Coupling' sections, such as evolution of the mean state, processes intrinsic to natural climate variability or local-scale effects (Xiao *et al.*, 2022; Ghosh and Shepherd, 2023). As a result, projections may offer too broad a range of potential outcomes, which could reduce their overall reliability.

Conclusion

In this review, I have provided an insight into various components associated with past, including relatively recent, research into the meteorology observed across the MC. This research is crucial given the risks posed to communities in the region due to extreme rainfall. There are several key processes influencing rainfall patterns over the MC, including the diurnal cycle and larger-scale modes of variability, such as the MJO, ENSO, IOD and equatorial waves. These processes interact with one another, complicating our understanding of regional precipitation patterns, further impacted by more synoptic-scale and transient processes. These interactions cannot be generalised for the entirety of the region, with studies requiring to focus on particular constituent islands within the archipelago.

The resultant limitations in our knowledge of meteorological processes in the MC, as well as the inherent difficulty in predicting convection, mean that systematic biases exist in the simulation of precipitation here. These biases have been addressed through significant efforts in improving the way in which we model convection, a function of the increase in computational power overtime. Increasing the horizontal resolution within simulations allows us to better visualise island-specific processes, which are sensitive to the representation of complex topography in the region. Removing the requirement for parametrisation of various processes also gives a more realistic representation of convection. The unique geographical configuration of the MC means that coupling to the ocean helps to correct air-sea interactions, such as surface heat flux exchange, which affect convective processes.

However, even with these developments in modelling capabilities, the representation of precipitation and convection continues to deviate away from observations. The requirement for better representation of key processes will also be crucial for future projections of MC rainfall, given the potential for significant shifts in the nature of convection across the region. We remain dependent on newer observations to help inform us on the finer-scale, complex interactions that significantly influence the environmental state of the MC. In turn, these observations would provide insight into the components within existing models that need readdressing, particularly sub-grid processes that often remain parameterised. The advent of sub-kilometre modelling approaches across the Tropics will inevitably prove beneficial for better representation of convection, which may be coupled with more intensive statistical and machine learning approaches. These approaches may help with analysing features previously difficult to pick out from non-linear, higher-order variability and complex relationships between a range of environmental parameters in the region.

Away from the technicalities of research, continued collaboration between scientists and stakeholders based in the MC remains paramount. Effective transfer of knowledge will highlight which components of the climate system are of priority to understand, primarily for local-to-regional numerical weather prediction. Such prioritisation of research tasks will assist in formulating action plans for tackling the vulnerabilities faced by communities across the region, exacerbated by frequent storm activity.

Acknowledgements

Aslam is funded by NERC through a SENSE CDT studentship (NE/T00039X/1), and would like to thank two anonymous reviewers for helping to improve the manuscript.

Data Availability Statement

Openly available datasets used in this analysis are available through the following links: ERA5 (https://cds.climate.copernicus.eu/), monthly Ocean Niño Index (ONI) for ENSO (https://origin.cpc.ncep.noaa.gov/products/analysis_monitoring/ensostuff/ONI_v5.php), monthly Dipole Mode Index (DMI) for IOD (https://psl.noaa.gov/data/timeseries/month/DMI/). All datasets were last accessed on 9 April 2025. Daily Real-time Multivariate (RMM) MJO index and IMERG GPM rainfall data were accessed via the Faculty of Environment servers at the University of Leeds. MJO RMM1 and RMM2 data (Wheeler and Hendon, 2004) are used to define the active phase of the MJO, where if the amplitude $\sqrt{RMM1^2 + RMM2^2}$ exceeds 1, an MJO event occurs. ONI data for ENSO are derived from the average sea surface temperature anomaly of the central-eastern tropical Pacific. DMI data for IOD are derived from the anomalous sea-surface temperature gradient between the western equatorial and southeastern equatorial Indian Ocean. Both ONI and DMI data are broadcast to daily equivalents and later smoothed with a 31-day running mean. El Niño events are defined for days where ONI is ≥0.5°C, and La Niña events are defined where ONI is ≤−0.5°C. Positive IOD events are defined for days where DMI is ≥0.2°C, and negative IOD events are defined where DMI is ≤−0.2°C.

References

Adames AF, **Maloney ED**. 2021. Moisture mode theory's contribution to advances in our understanding of the Madden-Julian Oscillation and other tropical disturbances. *Curr. Clim. Chang. Rep.* **7**: 72–85.

Adames AF, **Wallace JM**. 2015. Three-dimensional structure and evolution of the moisture field in the MJO. *J. Atmos. Sci.* **72**: 3733–3754.

Ajayamohan RS, **Khouider B**, **Praveen V** *et al*. 2021. Role of diurnal cycle in the maritime continent barrier effect on MJO propagation in an AGCM. *J. Atmos. Sci.* **78**: 1545–1565.

Argüeso D, **Romero R**, **Homar V**. 2020. Precipitation features of the maritime continent in parameterized and explicit convection models. *J. Clim.* **33**: 2449–2466.

As-syakur AR, **Tanaka T**, **Osawa T** *et al*. 2013. Indonesian rainfall variability observation using TRMM multi-satellite data. *Int. J. Remote Sens.* **34**: 7723–7738.

Baranowski DB, **Flatau MK**, **Flatau PJ** *et al*. 2016. Phase locking between atmospheric convectively coupled equatorial Kelvin waves and the diurnal cycle of precipitation over the Maritime Continent. *Geophys. Res. Lett.* **43**: 8269–8276.

Bernie DJ, **Guilyardi E**, **Madec G** *et al*. 2007. Impact of resolving the diurnal cycle in an ocean-atmosphere GCM. Part 1: a diurnally forced OGCM. *Clim. Dyn.* **29**: 575–590.

Bernie DJ, **Guilyardi E**, **Madec G** *et al*. 2008. Impact of resolving the diurnal cycle in an ocean-atmosphere GCM. Part 2: a diurnally coupled CGCM. *Clim. Dyn.* **31**: 909–925.

Birch CE, **Webster S**, **Peatman SC** *et al*. 2016. Scale interactions between the MJO and the western Maritime Continent. *J. Clim.* **29**: 2471–2492.

Chen C, **Sahany S**, **Moise AF** *et al*. 2023. ENSO–rainfall teleconnection over the maritime continent enhances and shifts eastward under warming. *J. Clim.* **36**: 4635–4663.

Chen G, **Wang B**. 2019. Dynamic moisture mode versus moisture mode in MJO dynamics: importance of the wave feedback and boundary layer convergence feedback. *Clim. Dyn.* **52**: 5127–5143.

DeMott CA, **Klingaman NP**, **Tseng WL** *et al*. 2019. The convection connection: how ocean feedbacks affect tropical mean moisture and MJO propagation. *J. Geophys. Res. -Atmos* **124**: 11910–11931.

Ferrett S, **Frame TH**, **Methven J** *et al*. 2021. Evaluating convection-permitting ensemble forecasts of precipitation over Southeast Asia. *Weather Forecast.* **36**: 1199–1217.

Ferrett S, **Yang GY**, **Woolnough SJ** *et al*. 2020. Linking extreme precipitation in Southeast Asia to equatorial waves. *Q. J. R. Meteorol. Soc.* **146**: 665–684.

Geng B, **Katsumata M**, **Taniguchi K**. 2020. Modulation of the diurnal cycle of precipitation near the southwestern coast of Sumatra by mixed Rossby-gravity waves. *J. Meteorol. Soc. Jpn.* **98**: 463–480.

Ghosh R, **Shepherd TG**. 2023. Storylines of Maritime Continent dry period precipitation changes under global warming. *Environ. Res. Lett.* **18**(3): 1–10.

Gill A. 1980. Some simple solutions for heat-induced tropical circulation. *Q. J. R. Meteorol. Soc.* **106**: 447–462.

Hardy S, **Methven J**, **Schwendike J** *et al*. 2023. Examining the dynamics of a Borneo vortex using a balance approximation tool. *Weather Clim. Dyn.* **4**: 1019–1043.

Hassim ME, **Lane TP**, **Grabowski WW**. 2016. The diurnal cycle of rainfall over New Guinea in convection-permitting WRF simulations. *Atmos. Chem. Phys.* **16**: 161–175.

Haylock M, **McBride J**. 2001. Spatial coherence and predictability of Indonesian Wet season rainfall. *J. Clim.* **14**: 3882–3887.

Hendon HH. 2003. Indonesian rainfall variability: impacts of ENSO and local air-sea interaction. *J. Clim.* **16**: 1775–1790.

Hendon HH, **Glick J**. 1997. Intraseasonal air-sea interaction in the Tropical Indian and Pacific Oceans. *J. Clim.* **10**: 647–661.

Hendon HH, **Salby ML**. 1994. The life cycle of the Madden–Julian Oscillation. *Am. Meteorol. Soc.* **51**: 2225–2237.

Hersbach H, **Bell B**, **Berrisford P** *et al*. 2020. The ERA5 global reanalysis. *Q. J. R. Meteorol. Soc.* **146**: 1999–2049.

Holloway CE, **Woolnough SJ**, **Lister GM**. 2012. Precipitation distributions for explicit versus parametrized convection in a large-domain high-resolution tropical case study. *Q. J. R. Meteorol. Soc.* **138**: 1692–1708.

Holloway CE, **Woolnough SJ**, **Lister GMS**. 2013. The effects of explicit versus parameterized convection on the MJO in a large-domain high-resolution tropical case study. Part I: characterization of large-scale organization and propagation. *J. Atmos. Sci.* **70**: 1342–1369.

Hsu J, **Chen CA**, **Lan CW** *et al*. 2025. Impact of land use changes and global warming on extreme precipitation patterns in the Maritime Continent. *NPJ Clim. Atmos. Sci.* **8**(5): 1–8.

Huffman GJ Bolvin DT Braithwaite D *et al*. 2020. NASA Global Precipitation Measurement (GPM) Integrated Multi-satellitE Retrievals for GPM (IMERG): Algorithm Theoretical Basis Document (ATBD) version 06. https://gpm.nasa.gov/sites/default/files/document_files/IMERG_ATBD_V06.pdf [Accessed 1 May 2025].

Jia XJ, **Ge JW**, **Wang S**. 2016. Diverse impacts of ENSO on wintertime rainfall over the Maritime Continent. *Int. J. Climatol.* **36**: 3384–3397.

Jin F, **Hoskins BJ**. 1995. The direct response to tropical heating in a Baroclinic atmosphere. *J. Atmos. Sci.* **52**: 307–319.

Kang S, **Im ES**, **Eltahir EA**. 2019. Future climate change enhances rainfall seasonality in a regional model of western Maritime Continent. *Clim. Dyn.* **52**: 747–764.

Karlowska E, **Matthews AJ**, **Webber BG** *et al*. 2024. Two-way feedback between the Madden–Julian Oscillation and diurnal warm layers in a coupled ocean–atmosphere model. *Q. J. R. Meteorol. Soc.* **150**: 4113–4132.

Klingaman NP, **DeMott CA**. 2020. Mean state biases and interannual variability affect perceived sensitivities of the Madden-Julian Oscillation to air-sea coupling. *J. Adv. Model Earth Syst.* **12**: e2019MS001799.

Klingaman NP, **Woolnough SJ**. 2014. The role of air-sea coupling in the simulation of the Madden-Julian Oscillation in the Hadley Centre model. *Q. J. R. Meteorol. Soc.* **140**: 2272–2286.

Koh T-Y, **Teo C-K**. 2009. Toward a mesoscale observation network in Southeast Asia. *Bull. Am. Meteorol. Soc.* **90**: 481–488.

Koseki S, **Koh TY**, **Teo CK**. 2013. Effects of the cold tongue in the South China Sea on the monsoon, diurnal cycle and rainfall in the Maritime Continent. *Q. J. R. Meteorol. Soc.* **139**: 1566–1582.

Latos B, **Lefort T**, **Flatau MK** *et al*. 2021. Equatorial waves triggering extreme rainfall and floods in southwest Sulawesi, Indonesia. *Mon. Weather Rev.* **149**: 1381–1401.

Latos B, **Peyrillé P**, **Lefort T** *et al*. 2023. The role of tropical waves in the genesis of Tropical Cyclone Seroja in the Maritime Continent. *Nat. Commun.* **14**: 1–12.

Li D, **Chen Y**, **Messmer M** *et al*. 2022. Compound wind and precipitation extremes across the Indo-Pacific: climatology, variability, and drivers. *Geophys. Res. Lett.* **49**: e2022GL098594.

Li X, **Lu R**, **Chen G** *et al*. 2024. Western North Pacific tropical cyclones suppress Maritime Continent rainfall. *NPJ Clim. Atmos. Sci.* **7**: 1–8.

Li X, **Wang X**, **Babovic V**. 2018. Analysis of variability and trends of precipitation extremes in Singapore during 1980–2013. *Int. J. Climatol.* **38**: 125–141.

Li Y, **Gupta AS**, **Taschetto AS** *et al*. 2020. Assessing the role of the ocean–atmosphere coupling frequency in the western Maritime Continent rainfall. *Clim. Dyn.* **54**: 4935–4952.

Li Y, **Jourdain NC**, **Taschetto AS** *et al*. 2017. Resolution dependence of the simulated precipitation and diurnal cycle over the Maritime Continent. *Clim. Dyn.* **48**: 4009–4028.

Liang S, **Wang D**, **Ziegler AD** *et al*. 2022. Madden–Julian Oscillation-induced extreme rainfalls constrained by global warming mitigation. *NPJ Clim. Atmos. Sci.* **5**: 1–9.

Love BS, **Matthews AJ**, **Lister GM**. 2011. The diurnal cycle of precipitation over the Maritime Continent in a high-resolution atmospheric model. *Q. J. R. Meteorol. Soc.* **137**: 934–947.

Lu J, **Li T**, **Shen X**. 2023. Precipitation diurnal cycle over the maritime continent modulated by ENSO. *Clim. Dyn.* **61**: 2547–2564.

Ma L, **Jiang Z**. 2021. Reevaluating the impacts of oceanic vertical resolution on the simulation of Madden–Julian Oscillation eastward propagation in a climate system model. *Clim. Dyn.* **56**: 2259–2278.

Madden RA, **Julian PR**. 1994. Observations of the 40–50-day tropical Oscillation – a review. *Mon. Weather Rev.* **122**: 814–837.

Majda AJ, **Stechmann SN**. 2009. A simple dynamical model with features of convective momentum transport. *J. Atmos. Sci.* **66**: 373–392.

Maloney ED, **Hartmann DL**. 1998. Frictional moisture convergence in a composite life cycle of the Madden-Julian Oscillation. *J. Clim.* **11**: 2387–2403.

Matsuno T. 1966. Quasi-geostrophic motions in the equatorial area. *J. Meteorol. Soc. Jpn.* **44**: 25–43.

Matthews AJ. 2000. Propagation mechanisms for the Madden-Julian Oscillation. *Q. J. R. Meteorol. Soc.* **126**: 2637–2651.

McPhaden MJ, **Zebiak SE**, **Glantz MH**. 2006. ENSO as an integrating concept in earth science. *Science* **314**: 1740–1745.

Mori S, **Jun-Ichi H**, **Yamanaka MD** *et al*. 2004. Diurnal land-sea rainfall peak migration over Sumatera Island, Indonesian Maritime Continent, observed by TRMM satellite and intensive rawinsonde soundings. *Mon. Weather Rev.* **132**: 2021–2039.

Mustafa JM, **Matthews AJ**, **Hall RA** *et al*. 2024. Characterisation of the observed diurnal cycle of precipitation over the Maritime Continent. *Q. J. R. Meteorol. Soc.* **150**: 2602–2624.

Neale R, **Slingo J**. 2003. The maritime continent and its role in the global climate: a GCM study. *J. Clim.* **16**: 834–848.

Nesbitt SW, **Zipser EJ**. 2003. The diurnal cycle of rainfall and convective intensity according to three years of TRMM measurements. *J. Clim.* **16**: 1456–1475.

Ngai ST, **Juneng L**, **Tangang F** *et al*. 2022. Projected mean and extreme precipitation based on bias-corrected simulation outputs of CORDEX Southeast Asia. *Weather Clim. Extreme* **37**: 100484.

Oh JH, **Kim KY**, **Lim GH**. 2012. Impact of MJO on the diurnal cycle of rainfall over the western Maritime Continent in the austral summer. *Clim. Dyn.* **38**: 1167–1180.

Okugawa R, **Yasunaga K**, **Hamada A** *et al*. 2024. Numerical study on the precipitation concentration over the western coast of Sumatra Island. *Mon. Weather Rev.* **152**: 689–704.

Pearson KJ, **Lister GM**, **Birch CE** *et al*. 2014. Modelling the diurnal cycle of tropical convection across the 'grey zone'. *Q. J. R. Meteorol. Soc.* **140**: 491–499.

Peatman SC, **Birch CE**, **Schwendike J** *et al*. 2023. The role of density currents and gravity waves in the offshore propagation of convection over Sumatra. *Mon. Weather Rev.* **151**: 1757–1777.

Peatman SC, **Matthews AJ**, **Stevens DP**. 2014. Propagation of the Madden-Julian Oscillation through the Maritime Continent and scale interaction with the diurnal cycle of precipitation. *Q. J. R. Meteorol. Soc.* **140**: 814–825.

Peatman SC, **Schwendike J**, **Birch CE** *et al*. 2021. A local-to-large scale view of Maritime Continent rainfall: control by ENSO, MJO and equatorial waves. *J. Clim.* **34**: 8933–8953.

Pegion K, **Kirtman BP**. 2008. The impact of air-sea interactions on the simulation of tropical intraseasonal variability. *J. Clim.* **21**: 6616–6635.

Qian JH. 2008. Why precipitation is mostly concentrated over islands in the Maritime Continent. *J. Atmos. Sci.* **65**: 1428–1441.

Rashid HA, **Hirst AC**. 2017. Mechanisms of improved rainfall simulation over the Maritime Continent due to increased horizontal resolution in an AGCM. *Clim. Dyn.* **49**: 1747–1764.

Rauniyar SP, **Walsh KJ**. 2013. Influence of ENSO on the diurnal cycle of rainfall over the Maritime Continent and Australia. *J. Clim.* **26**: 1304–1321.

Raymond DJ, **Fuchs Z**. 2009. Moisture modes and the Madden-Julian Oscillation. *J. Clim.* **22**: 3031–3046.

Ridout JA, **Flatau MK**. 2011. Convectively coupled Kelvin wave propagation past Sumatra: a June case and corresponding composite analysis. *J. Geophys. Res. Atmos.* **116**: D07106.

Saji N, **Goswami B**, **Vinayachandran P** *et al*. 1999. A dipole mode in the tropical Indian Ocean. *Nature* **401**: 360–363.

Saji N, **Yamagata T**. 2003. Possible impacts of Indian Ocean Dipole mode events on global climate. *Clim. Res.* **25**: 151–169.

Sakaeda N, **Kiladis G**, **Dias J**. 2020. The diurnal cycle of rainfall and the convectively coupled equatorial waves over the Maritime Continent. *J. Clim.* **33**: 3307–3331.

Satomura T. 2000. Diurnal variation of precipitation over the Indo-China Peninsula: two-dimensional numerical simulation. *J. Meteorol. Soc. Japan* **78**: 461–475.

Schiemann R, **Demory ME**, **Mizielinski MS** *et al*. 2014. The sensitivity of the tropical circulation and Maritime Continent precipitation to climate model resolution. *Clim. Dyn.* **42**: 2455–2468.

Scoccimarro E, **Gualdi S**, **Bellucci A** *et al*. 2020. The typhoon-induced drying of the Maritime Continent. *PNAS* **117**: 3983–3988.

Senior NV, **Matthews AJ**, **Webber BG** *et al*. 2023. Extreme precipitation at Padang, Sumatra triggered by convectively coupled Kelvin waves. *Q. J. R. Meteorol. Soc.* **149**: 2281–2300.

Sobel A, **Maloney E**. 2013. Moisture modes and the Eastward propagation of the MJO. *J. Atmos. Sci.* **70**: 187–192.

Su CY, **Wu CM**, **Chen WT** *et al*. 2022. The effects of the unified parameterization in the CWBGFS: the diurnal cycle of precipitation over land in the Maritime Continent. *Clim. Dyn.* **58**: 223–233.

Supari Tangang F, **Juneng L**, **Cruz F** *et al*. 2020. Multi-model projections of precipitation extremes in Southeast Asia based on CORDEX-Southeast Asia simulations. *Environ. Res.* **184**: 109350.

Takahashi HG. 2011. Long-term changes in rainfall and tropical cyclone activity over South and Southeast Asia. *Adv. Geosci.* **30**: 17–22.

Tan H, **Ray P**, **Barrett B** *et al*. 2021. Systematic patterns in land precipitation due to convection in Neighboring islands in the Maritime Continent during MJO propagation. *J. Geophys. Res. Atmos.* **126**: e2020JD033465.

Tangang F, **Chung JX**, **Juneng L** *et al*. 2020. Projected future changes in rainfall in Southeast Asia based on CORDEX–SEA multi-model simulations. *Clim. Dyn.* **55**: 1247–1267.

Torti JM. 2012. Floods in Southeast Asia: a health priority. *J. Glob. Health* **2**(2): 020304.

Vincent CL, **Lane TP**. 2016. Evolution of the diurnal precipitation cycle with the passage of a Madden-Julian Oscillation event through the Maritime Continent. *Mon. Weather Rev.* **144**: 1983–2005.

Wang B, **Liu F**, **Chen G**. 2016. A trio-interaction theory for Madden–Julian Oscillation. *Geosci. Lett.* **3**: 1–16.

Wang L, **Li T**. 2020. Reexamining the MJO moisture mode theories with normalized phase evolutions. *J. Clim.* **33**: 8523–8536.

Warner TT, **Mapes BE**, **Xu M**. 2003. Diurnal patterns of rainfall in Northwestern South America. Part II: model simulations. *Mon. Weather Rev.* **131**: 813–829.

Wheeler M, **Kiladis GN**. 1999. Convectively coupled equatorial waves: analysis of clouds and temperature in the wavenumber-frequency domain. *J. Atmos. Sci.* **56**: 374–399.

Wheeler MC, **Hendon HH**. 2004. An all-season real-time multivariate MJO Index: development of an index for monitoring and prediction. *Mon. Weather Rev.* **132**: 1917–1932.

Wijayanti P, **Zhu X**, **Hellegers P** *et al*. 2017. Estimation of river flood damages in Jakarta, Indonesia. *Nat. Hazards* **86**: 1059–1079.

Woolnough SJ, **Slingo JM**, **Hoskins BJ**. 2000. The relationship between convection and sea surface temperature on intraseasonal timescales. *J. Clim.* **13**: 2086–2104.

Woolnough SJ, **Slingo JM**, **Hoskins BJ**. 2001. The organization of tropical convection by intraseasonal sea surface temperature anomalies. *Q. J. R. Meteorol. Soc.* **127**: 887–907.

Xiao HM, **Lo MH**, **Yu JY**. 2022. The increased frequency of combined El Niño and positive IOD events since 1965s and its impacts on Maritime Continent hydroclimates. *Sci. Rep.* **12**: 1–10.

Xue P, **Malanotte-Rizzoli P**, **Wei J** *et al*. 2020. Coupled ocean-atmosphere modeling over the Maritime continent: a review. *J. Geophys. Res. Oceans* **125**: e2019JC014978.

Yamanaka MD. 2016. Physical climatology of Indonesian maritime continent: an outline to comprehend observational studies. *Atmos. Res.* **178-179**: 231–259.

Yamanaka MD, **Ogino SY**, **Wu PM** *et al*. 2018. Maritime continent coastlines controlling Earth's climate. *Prog Earth Planet Sci* **5**: 1–28.

Yang D, **Ingersoll AP**. 2013. Triggered convection, gravity waves, and the MJO: a shallow-water model. *J. Atmos. Sci.* **70**: 2476–2486.

Yang G-Y, **Hoskins B**, **Slingo J**. 2003. Convectively coupled equatorial waves: a new methodology for identifying wave structures in observational data. *J. Atmos. Sci.* **60**: 1637–1654.

Yang G-Y, **Slingo J**. 2001. The diurnal cycle in the tropics. *Mon. Weather Rev.* **129**: 784–801.

Yokoi S, **Mori S**, **Katsumata M** *et al*. 2017. Diurnal cycle of precipitation observed in the western coastal area of Sumatra Island: offshore preconditioning by gravity waves. *Mon. Weather Rev.* **145**: 3745–3761.

Zhang C. 2005. Madden-Julian Oscillation. *Rev. Geophys.* **43**: 1–36.

Zhang C, **Adames F**, **Khouider B** *et al*. 2020. Four theories of the Madden-Julian Oscillation. *Rev. Geophys.* **58**: e2019RG000685.

Correspondence to: A. A. Aslam
eeaaas@leeds.ac.uk

doi: 10.1002/wea.7731